Supplementary Information:
An analytical model for antiambipolar behavior in organic electrochemical transistors

Marcos Luginieski[1,2,3,*], Bruno Bassi Millan Torres[1], Bianca de Andrade Feitosa[1], Henrique Frulani de Paula Barbosa[1], Björn Lüssem[2,3], and Gregório Couto Faria[1,†]

[1]São Carlos Institute of Physics, University of São Paulo, PO Box 369, 13560-970, São Carlos, SP, Brazil
[2]Institute for Microsensors, Actuators and Systems, University of Bremen, 28359 Bremen, Germany
[3]MAPEX – Center for Materials and Processes, University of Bremen, 28359 Bremen, Germany
[*]EMAIL: mluginieski@ifsc.usp.br
[†]EMAIL: gcfaria@ifsc.usp.br

S-1 Model of an n-type OECT

S-1.1 Mathematical development

The model developed here is based on our previous publication by Feitosa et al.[1]. For n-type semiconductors, the redox reaction inside the channel can be written as[1]

$$O_x^o + e^- \rightleftharpoons R_{ed}^-.$$

To account for the two reduction peaks observed in CV curves of BBL and the existence of multiply charged species[2], we propose the following electrochemical equations:

$$O_x^0 + e^- \rightleftharpoons R_{ed}^- \tag{S1}$$
$$R_{ed}^- + e^- \rightleftharpoons R_{ed}^{2-}, \tag{S2}$$

where R_{ed}^{2-} is a second reduced state with charge $2-$.

The formation of a double charge is shown in Fig. S1, where *in situ* spectroelectrochemical and chronoamperometry experiments are performed. During electrochemical doping, the peak at 580 nm, associated with the π–π^* transition, decreases in intensity as the film becomes increasingly doped. Concurrently, a broad band emerges in the 700–1000 nm region at negative potentials, and a pronounced peak develops between 400 and 500 nm. These spectral changes indicate that the energy bands of the film undergo significant modification during electrochemical doping.

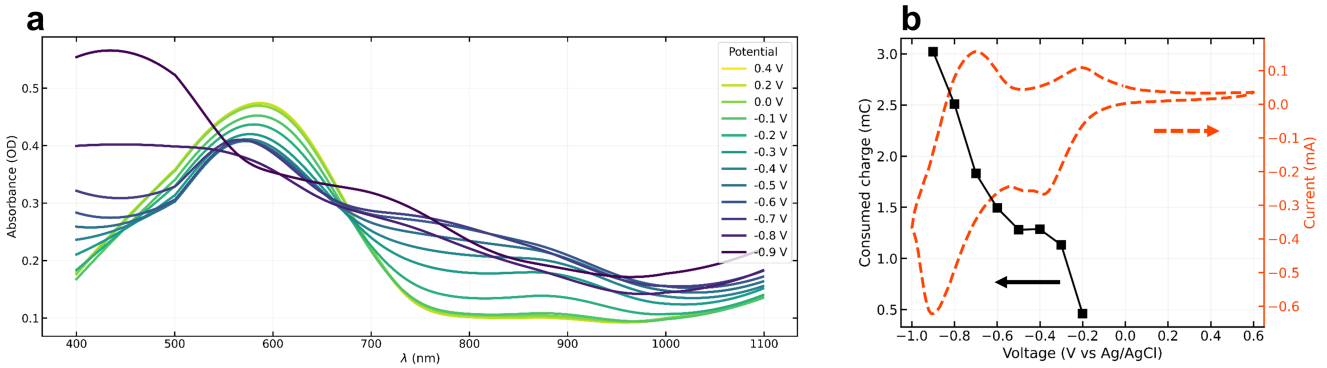

Figure S1. a. Absorption spectra of BBL/ITO thin film during electrochemical doping. **b.** CV curve (50 mV/s) and total charge calculated from chronoamperometry experiment. In both experiments, the electrolyte was 100 mM NaCl, Pt as counter electrode, and an Ag/AgCl pellet as pseudo-reference electrode.

In Fig. S1b, the CV curve is plotted alongside the total charge extracted from the chronoamperometry experiment. Notably, at the second peak (-0.9 V), nearly twice the charge associated with the first peak (-0.6 V) is consumed in the electrochemical process, reinforcing our hypothesis.

Again, we assume that channel/electrolyte/gate system forms an electrochemical cell[1], described by the Nernst equation

$$\Delta V_{meas} = \varepsilon_1 - \frac{RT}{F\gamma}\ln\frac{C_{R^-_{ed}}}{C_{O^0_x}} \qquad \& \qquad \Delta V_{meas} = \varepsilon_2 - \frac{RT}{F\gamma}\ln\frac{C_{R^{2-}_{ed}}}{C_{R^-_{ed}}}, \tag{S3}$$

where $\Delta V_{meas} = \varepsilon_{ch} - \varepsilon_G$ is the measured voltage across the electrochemical cell, ε_{ch} is the transistor's channel potential and ε_G is the gate electrode potential. Note that the variable ε denotes the electrode potential, incorporating both chemical and electrical contributions[1]. Furthermore, $C_{O^0_x}$, $C_{R^-_{ed}}$ and $C_{R^{2-}_{ed}}$ correspond to the concentration in mol/cm^3 of oxidized, singly and doubly reduced species, respectively, R is the universal gas constant, T is the temperature, F is Faraday's constant, γ is a non-ideality parameter. Finally, ε_1 and ε_2 are the formal electrode potential for the reduction reactions associated with the single and the double charges on the polymer chain, and can be defined as:

$$\varepsilon_1 = \varepsilon^{\ominus}_{pol,1} - \varepsilon_G \qquad \& \qquad \varepsilon_2 = \varepsilon^{\ominus}_{pol,2} - \varepsilon_G.$$

Both $\varepsilon^{\ominus}_{pol,1}$ and $\varepsilon^{\ominus}_{pol,2}$ are the standard electrode potentials for each reaction. See that, following the original paper[1]

$$\varepsilon_G = \varepsilon^{\ominus}_{Ag/AgCl} - \frac{RT}{F}\ln C_{Cl^-},$$

that is, the gate potential depends on the concentration of Cl^-.

Assuming that the maximum density of carriers is given to be the sum of all species, one has

$$\rho_{max} = C_{O^0_{ox}} + C_{R^-_{ed}} + C_{R^{2-}_{ed}} = \text{constant}$$

See that the number of charge carriers in the active layer, associated with each reaction process is given by: $C_{R^-_{ed}} = \rho_1$ and $C_{R^{2-}_{ed}} = \rho_2$. Therefore:

$$\rho_{max} = \rho_{O^0_{ox}} + \rho_1 + \rho_2. \tag{S4}$$

Plugging this equation into the above definitions of ΔV_{meas}, one has:

$$\Delta V_{meas} = \varepsilon_1 - \frac{RT}{F\gamma}\ln\frac{\rho_1}{\rho_{max} - \rho_1 - \rho_2} \qquad \& \qquad \Delta V_{meas} = \varepsilon_2 - \frac{RT}{F\gamma}\ln\frac{\rho_2}{\rho_1}. \tag{S5}$$

Following the assumptions of the original model, the OECT channel is taken as unidimensional, neglecting any ionic movement across the organic semiconductor, and the electronic mobility is taken as constant[1]. The measured potential can be written as a function of species distribution along the OECT channel. Therefore, ΔV_{meas} is rewritten in terms of the local potential for every position x, that is, $\Delta V_{x,G} = \varepsilon(x) - \varepsilon_G$. Again, to keep the notation simple, every function of x will be denoted by the suffix x. Then

$$-\frac{F\gamma}{RT}(\varepsilon_x - \varepsilon_G - \varepsilon_1) = \ln\frac{\rho_{1,x}}{\rho_{max} - \rho_{1,x} - \rho_{2,x}} \qquad \& \qquad -\frac{F\gamma}{RT}(\varepsilon_x - \varepsilon_G - \varepsilon_2) = \ln\frac{\rho_{2,x}}{\rho_{1,x}}$$

$$\exp\left[-\frac{F\gamma}{RT}(\varepsilon_x - \varepsilon_G - \varepsilon_1)\right] = \frac{\rho_{1,x}}{\rho_{max} - \rho_{1,x} - \rho_{2,x}} \qquad \& \qquad \exp\left[-\frac{F\gamma}{RT}(\varepsilon_x - \varepsilon_G - \varepsilon_2)\right] = \frac{\rho_{2,x}}{\rho_{1,x}}.$$

Let $\theta_{i,x} = \exp\left[-\frac{F\gamma}{RT}(\varepsilon_x - \varepsilon_G - \varepsilon_i)\right]$, for $i = 1, 2$, therefore

$$\theta_{1,x} = \frac{\rho_{1,x}}{\rho_{max} - \rho_{1,x} - \rho_{2,x}} \qquad \& \qquad \theta_{2,x} = \frac{\rho_{2,x}}{\rho_{1,x}},$$

then

$$\rho_{1,x} = \frac{(\rho_{max} - \rho_{2,x})\theta_{1,x}}{1 + \theta_{1,x}} \qquad \& \qquad \rho_{2,x} = \rho_{1,x}\theta_{2,x}.$$

Finally

$$\rho_{1,x} = \rho_{max}\frac{\theta_{1,x}}{1+\theta_{1,x}+\theta_{1,x}\theta_{2,x}} \qquad \& \qquad \rho_{2,x} = \rho_{max}\frac{\theta_{1,x}\theta_{2,x}}{1+\theta_{1,x}+\theta_{1,x}\theta_{2,x}}. \tag{S6}$$

To facilitate the following development, the density equations can be rewritten in terms of the applied potentials in an OECT. According to[1],

$$V_{GS} = \Delta V_{GS} = \varepsilon_G - \varepsilon_S \tag{S7}$$

and

$$V_{DS} = \Delta V_{DS} = \varepsilon_D - \varepsilon_S. \tag{S8}$$

We then define $V(x) = \varepsilon(x) - \varepsilon_S$. Rewriting $\theta_{i,x}$ yields

$$\theta_{i,x} = \exp\left[-\frac{F\gamma}{RT}\left(V_x - V_{GS} - \varepsilon_i\right)\right], \tag{S9}$$

for $i = 1, 2$. Note that this transformation is more than a simple change of variables; it corresponds to shifting the reference of the electrode potential to the source.

The total density $\rho_t = \rho_1 + \rho_2$ follows a sigmoid behavior (see Fig. S2) as already observed in the previous model[1].

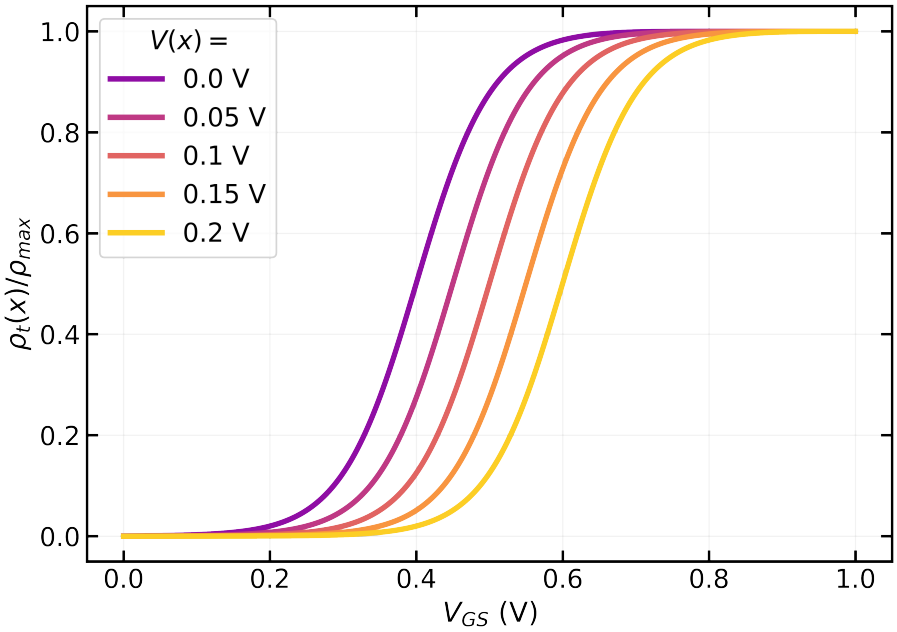

Figure S2. Total density ($\rho_t = \rho_1 + \rho_2$), calculated from Fig. 2a from the main paper.

By solving $d\rho_{1,x}/dV_{GS} = 0$ to V_{GS} leads to $\frac{1}{2}(2V_x - \varepsilon_1 - \varepsilon_2)$ being the potential where the maximum density of single carriers is reached.

Finally, the total channel current density can be described by Ohm's law, where

$$J_{DS} = J_1 + J_2, \tag{S10}$$

is a sum of the current associated with the two charges considered. Here, we evoke the gradual channel approximation, where it is assumed that the potential varies gradually between source and drain electrodes. Therefore, each term from Eq. (S10) is written as

$$J_{1,x} = -F\mu_1\rho_{1,x}\frac{dV_x}{dx} \tag{S11}$$

and

$$J_{2,x} = -2F\mu_2\rho_{2,x}\frac{dV_x}{dx}. \tag{S12}$$

The extra 2 term in the later equation accounts for the double charge associated with $C_{R_{ed}^{2-}}$ species.

S-1.1.1 Drain current

The total drain current I_{DS} can be obtained by plugging Eqs. (S6) into (S11) and (S12). The integration over the potential is carried out from 0 to V_{DS}, which correspond to the source and drain potentials, respectively. Let W, d, and L be the channel width, thickness, and length, then each current is given by:

$$\int_0^L I_1 dx = -WdF\mu_1\rho_{max}\int_0^{V_{DS}}\frac{\theta_{1,x}}{1+\theta_{1,x}+\theta_{1,x}\theta_{2,x}}dV_x,$$

and

$$\int_0^L I_2 dx = -2WdF\mu_2\rho_{max}\int_0^{V_{DS}}\frac{\theta_{1,x}\theta_{2,x}}{1+\theta_{1,x}+\theta_{1,x}\theta_{2,x}}dV_x.$$

Finally, after performing both integrations, one has:

$$I_1 = \frac{Wd}{L}\frac{\sigma_1}{\beta}\frac{2e^{\beta(\varepsilon_1+V_{GS})}}{\xi}\left[\operatorname{arctanh}(\Lambda_a)-\operatorname{arctanh}(\Lambda_b)\right] \tag{S13}$$

for the single charge current, and

$$I_2 = \frac{Wd}{L}\frac{\sigma_2}{\beta}\left\{-2\beta V_{DS}+\frac{2e^{\beta(\varepsilon_1+V_{GS})}\left[\operatorname{arctanh}(\Lambda_a)-\operatorname{arctanh}(\Lambda_b)\right]}{\xi}-\log(\Theta_a)+\log(\Theta_b)\right\} \tag{S14}$$

for the double charge current. Finally, the total drain current $I_{DS} = I_1 + I_2$ is given by:

$$\begin{aligned} I_{DS} = \frac{Wd}{L}\frac{1}{\beta\xi}\Big\{&2e^{\beta(\varepsilon_1+V_{GS})}(\sigma_2-\sigma_1)\left[-\operatorname{arctanh}(\Lambda_a)+\operatorname{arctanh}(\Lambda_b)\right]+\\ &+\sigma_2\xi\left[2\beta V_{DS}+\log(\Theta_a)-\log(\Theta_b)\right]\Big\}. \end{aligned} \tag{S15}$$

However, $\operatorname{arctanh}u - \operatorname{arctanh}v = \operatorname{arctanh}\frac{u-v}{1-uv}$, then Eqs. (S13)-(S15) can be rewritten as:

$$I_1 = \frac{Wd}{L}\frac{\sigma_1}{\beta}\frac{2e^{\beta(\varepsilon_1+V_{GS})}}{\xi}\operatorname{arctanh}(\Lambda_c), \tag{S16}$$

$$I_2 = \frac{Wd}{L}\frac{\sigma_2}{\beta}\left\{2\beta V_{DS}-\frac{2e^{\beta(\varepsilon_1+V_{GS})}\operatorname{arctanh}(\Lambda_c)}{\xi}+\log(\Theta_a)-\log(\Theta_b)\right\}, \tag{S17}$$

and, finally

$$\begin{aligned} I_{DS} = \frac{Wd}{L}\frac{1}{\beta}\Big\{&-\frac{2e^{\beta(\varepsilon_1+V_{GS})}(\sigma_2-\sigma_1)\operatorname{arctanh}(\Lambda_c)}{\xi}+\\ &+\sigma_2\left[2\beta V_{DS}+\log(\Theta_a)-\log(\Theta_b)\right]\Big\}, \end{aligned} \tag{S18}$$

where

$$\Lambda_c = \frac{\left(-1+e^{\beta V_{DS}}\right)\xi}{2e^{\beta V_{DS}}+e^{\beta(\varepsilon_1+V_{GS})}+e^{\beta(\varepsilon_1+V_{DS}+V_{GS})}+2e^{\beta(\varepsilon_1+\varepsilon_2+2V_{GS})}}. \tag{S19}$$

The definition of $\Lambda_a, \Lambda_b, \Theta_a, \Theta_b, \sigma_1, \sigma_2$, and ξ is summarized in Table S1. See that Eq. (S18) is more straightforward for implementing into simulations or fitting experimental data, while Eq. S15 is helpful to visualize the symmetry of the equation.

Table S1. List of simplified equations.

Variable	Definition
β	$\frac{F\gamma}{RT}$
σ_1	$F\mu_1\rho_{max}$
σ_2	$F\mu_2\rho_{max}$
ξ	$\sqrt{e^{2\beta(\varepsilon_1+V_{GS})}-4e^{\beta(\varepsilon_2+\varepsilon_1+2V_{GS})}}$
Λ_a	$\frac{2+e^{\beta(\varepsilon_1+V_{GS})}}{\xi}$
Λ_b	$\frac{2e^{\beta V_{DS}}+e^{\beta(\varepsilon_1+V_{GS})}}{\xi}$
Θ_a	$1+e^{\beta(\varepsilon_1+V_{GS})}+e^{\beta(\varepsilon_2+\varepsilon_1+2V_{GS})}$
Θ_b	$e^{2\beta V_{DS}}+e^{\beta(\varepsilon_1+V_{DS}+V_{GS})}+e^{\beta(\varepsilon_2+\varepsilon_1+2V_{GS})}$

For the above drain-current equations to have real solution, the radicand of ξ must be positive, otherwise ξ would be an imaginary number. Furthermore, it cannot be zero, since it is the denominator in Eq. (S18). Therefore:

$$\begin{aligned}
e^{2\beta(\varepsilon_1+V_{GS})}-4e^{\beta(\varepsilon_2+\varepsilon_1+2V_{GS})} &> 0\\
e^{\beta(\varepsilon_1+V_{GS})}\left[e^{\beta(\varepsilon_1+V_{GS})}-4e^{\beta(\varepsilon_2+V_{GS})}\right] &> 0\\
e^{\beta(\varepsilon_1+V_{GS})} &> 4e^{\beta(\varepsilon_2+V_{GS})}\\
\beta(\varepsilon_1+V_{GS}) &> \ln(4)+\beta(\varepsilon_2+V_{GS})\\
\varepsilon_1 &> \frac{\ln(4)}{\beta}+\varepsilon_2\\
\varepsilon_1-\varepsilon_2 &> \frac{\ln(4)}{\beta}\\
\Delta\varepsilon &> \frac{\ln(4)}{\beta}
\end{aligned}$$

or

$$\boxed{\Delta\varepsilon > \ln(4)\frac{V_T}{\gamma}}, \tag{S20}$$

where $\ln(4)V_T = \ln(4)\frac{RT}{F} = 35.62$ mV at $T = 298.15$ K. Taking $\gamma = 1.0$, $\Delta\varepsilon > 36$ mV. Since β is a positive constant, it follows that $|\varepsilon_1| < |\varepsilon_2|$ must always hold. This implies that ρ_1 should initially exceed ρ_2, as shown in Fig. 1a of the main manuscript. When $\varepsilon_2 \ll \varepsilon_1$, ρ_2 remains zero, while ρ_1 increases as expected before becoming unchanged at its maximum value. Therefore, by taking this limit and considering that $\mu_1 \gg \mu_2$ in Eq. (S18), it is possible to reduce the complexity of the equation without losing significant information about the system. The simplified drain current equation is then written as

$$\begin{aligned}
I_{DS,simp} &= \lim_{\sigma_2\to 0} I_{DS,full}\\
I_{DS,simp} = \lim_{\sigma_2\to 0}\frac{Wd}{L}\frac{1}{\beta}\Bigg\{ &-\frac{2e^{\beta(\varepsilon_1+V_{GS})}(\sigma_2-\sigma_1)\,\mathrm{arctanh}(\Lambda_c)}{\xi}+\\
&+\sigma_2\left[2\beta V_{DS}+\log(\Theta_a)-\log(\Theta_b)\right]\Bigg\},
\end{aligned}$$

which reduces simply to

$$I_{DS} = \frac{Wd}{L}\frac{\sigma_1}{\beta}\frac{2e^{\beta(\varepsilon_1+V_{GS})}}{\xi}\,\mathrm{arctanh}(\Lambda_c). \tag{S21}$$

S-1.1.2 Transconductance

Given that $g_m = \frac{\partial I_{DS}}{\partial V_{GS}}$, then, from Eq. (S21):

$$g_m = \frac{Wd}{L}\sigma_1 \frac{e^{\beta(\varepsilon_1+V_{GS})}\left(e^{\beta V_{DS}}-1\right)\left[e^{\beta V_{DS}}-e^{\beta(\varepsilon_2+\varepsilon_1+2V_{GS})}\right]}{\Theta_a\Theta_b}. \tag{S22}$$

The gate voltage where maximum drain current is achieved can be determined by taking $g_m = 0$. Solving it for V_{GS}, one has

$$V_{GS,max} = \frac{1}{2}\left[V_{DS}-(\varepsilon_2+\varepsilon_1)\right]. \tag{S23}$$

Finally, the channel conductance can be defined as $g_d = \frac{\partial I_{DS}}{\partial V_{DS}}$. Then, from Eq. (S21), one has

$$g_d = \frac{Wd}{L}\sigma_1 \frac{e^{\beta(\varepsilon_1+V_{DS}+V_{GS})}}{\Theta_b}. \tag{S24}$$

S-2 Model of a p-type OECT

For p-type semiconductors, we have:

$$O_{ox}^{+} + e^{-} \rightleftharpoons R_{ed}^{0} \tag{S25}$$
$$O_{ox}^{2+} + e^{-} \rightleftharpoons O_{ox}^{+}, \tag{S26}$$

where O_{ox}^{2+} is a second oxidize state with charge 2+.

Again, the voltage difference across the electrochemical cell is

$$\Delta V_{meas} = \varepsilon_1 - \frac{RT}{F\gamma}\ln\frac{C_{R_{ed}^0}}{C_{O_{ox}^+}} \qquad \& \qquad \Delta V_{meas} = \varepsilon_2 - \frac{RT}{F\gamma}\ln\frac{C_{O_{ox}^+}}{C_{O_{ox}^{2+}}}, \tag{S27}$$

Assuming that the maximum density of carriers is given to be the sum of all species, one has

$$\begin{aligned}\rho_{max} &= C_{R_{ed}^0} + C_1 + C_2 \\ &= \rho_{R_{ed}^0} + \rho_1 + \rho_2.\end{aligned} \tag{S28}$$

Note that, in this case $C_{O_{ox}^+} = C_1$ and $C_{O_{ox}^{2+}} = C_2$. Then

$$\Delta V_{meas} = \varepsilon_1 - \frac{RT}{F\gamma}\ln\frac{\rho_{max} - \rho_1 - \rho_2}{\rho_1} \qquad \& \qquad \Delta V_{meas} = \varepsilon_2 - \frac{RT}{F\gamma}\ln\frac{\rho_1}{\rho_2}. \tag{S29}$$

Following the same steps done for n-type model, the final charge density equations become:

$$\rho_{1,x} = \rho_{max}\frac{\theta_{2,x}}{1 + \theta_{2,x} + \theta_{1,x}\theta_{2,x}} \qquad \& \qquad \rho_{2,x} = \rho_{max}\frac{1}{1 + \theta_{2,x} + \theta_{1,x}\theta_{2,x}}. \tag{S30}$$

These equations lead to the same trade-off between single and doubly charged species density seen for n-type materials. Finally, following Eqs. (S11) and (S12), performing the integration and following the same steps, one has:

$$I_1 = \frac{Wd}{L}\frac{\sigma_1}{\beta}\frac{2e^{\beta(\varepsilon_2+V_{GS})}}{\xi_p}\operatorname{arctanh}(\Lambda_p), \tag{S31}$$

$$I_2 = \frac{Wd}{L}\frac{\sigma_2}{\beta}\left\{-\frac{2e^{\beta(\varepsilon_2+V_{GS})}\operatorname{arctanh}(\Lambda_p)}{\xi_p} - \log(\Theta_{a,p}) + \log(\Theta_{b,p})\right\}, \tag{S32}$$

and, finally

$$I_{DS} = \frac{Wd}{L}\frac{1}{\beta}\left\{-\frac{2e^{\beta(\varepsilon_2+V_{GS})}(\sigma_2 - \sigma_1)\operatorname{arctanh}(\Lambda_p)}{\xi_p} + \sigma_2\left[-\log(\Theta_{a,p}) + \log(\Theta_{b,p})\right]\right\}. \tag{S33}$$

New terms are depicted in Table S2.

Table S2. List of simplified equations for the p-type case.

Variable	Definition
ξ_p	$\sqrt{e^{2\beta(\varepsilon_2+V_{GS})} - 4e^{\beta(\varepsilon_2+\varepsilon_1+2V_{GS})}}$
λ_p	$\frac{\left(-1+e^{\beta V_{DS}}\right)\xi_p}{2e^{\beta V_{DS}}+e^{\beta(\varepsilon_2+V_{GS})}+e^{\beta(\varepsilon_2+V_{DS}+V_{GS})}+2e^{\beta(\varepsilon_1+\varepsilon_2+2V_{GS})}}$
$\Theta_{a,p}$	$1 + e^{\beta(\varepsilon_2+V_{GS})} + e^{\beta(\varepsilon_2+\varepsilon_1+2V_{GS})}$
$\Theta_{b,p}$	$e^{2\beta V_{DS}} + e^{\beta(\varepsilon_2+V_{DS}+V_{GS})} + e^{\beta(\varepsilon_2+\varepsilon_1+2V_{GS})}$

See that, again, considering $\mu_1 \gg \mu_p$ leads to $I_{DS} = I_1$. For this case, transconductance is written as

$$g_m = \frac{Wd}{L}\sigma_1 \frac{e^{\beta(\varepsilon_2+V_{GS})}\left(e^{\beta V_{DS}}-1\right)\left[e^{\beta V_{DS}}-e^{\beta(\varepsilon_2+\varepsilon_1+2V_{GS})}\right]}{\Theta_{a,p}\Theta_{b,p}}. \tag{S34}$$

Again, solving $g_m = 0$ to V_{GS}, one has the same Eq. (S23). The conductance is given by

$$g_d = \frac{Wd}{L}\sigma_1 \frac{e^{\beta(\varepsilon_2+V_{DS}+V_{GS})}}{\Theta_{b,p}}. \tag{S35}$$

See that, because of ξ_p, $\Delta\varepsilon$ is defined as $\varepsilon_2 - \varepsilon_1$ for this case. The inequality, however, remains the same.

S-3 vOECT performance

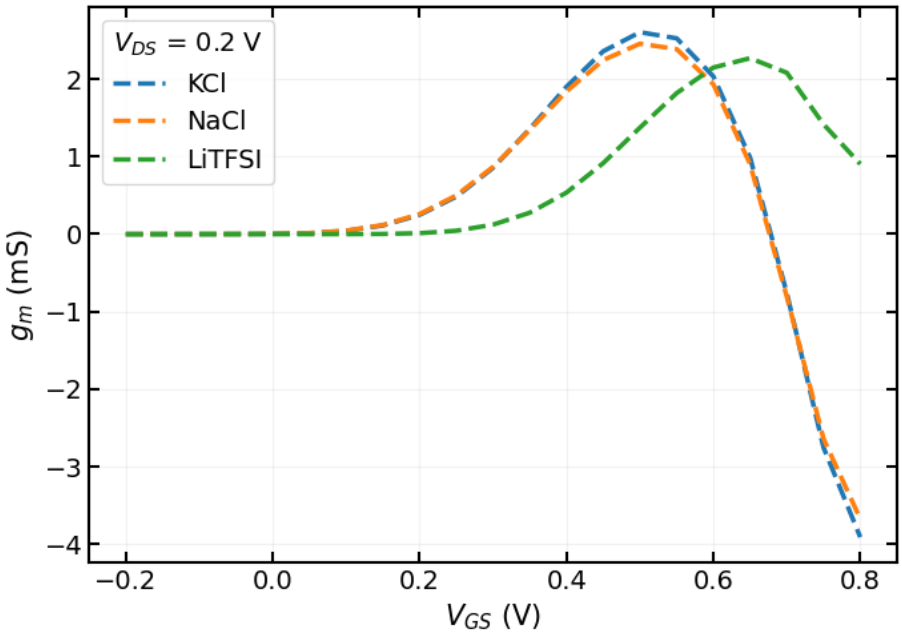

Figure S3. Transconductance from vOECTs from Fig. 3c.

S-4 Fitting

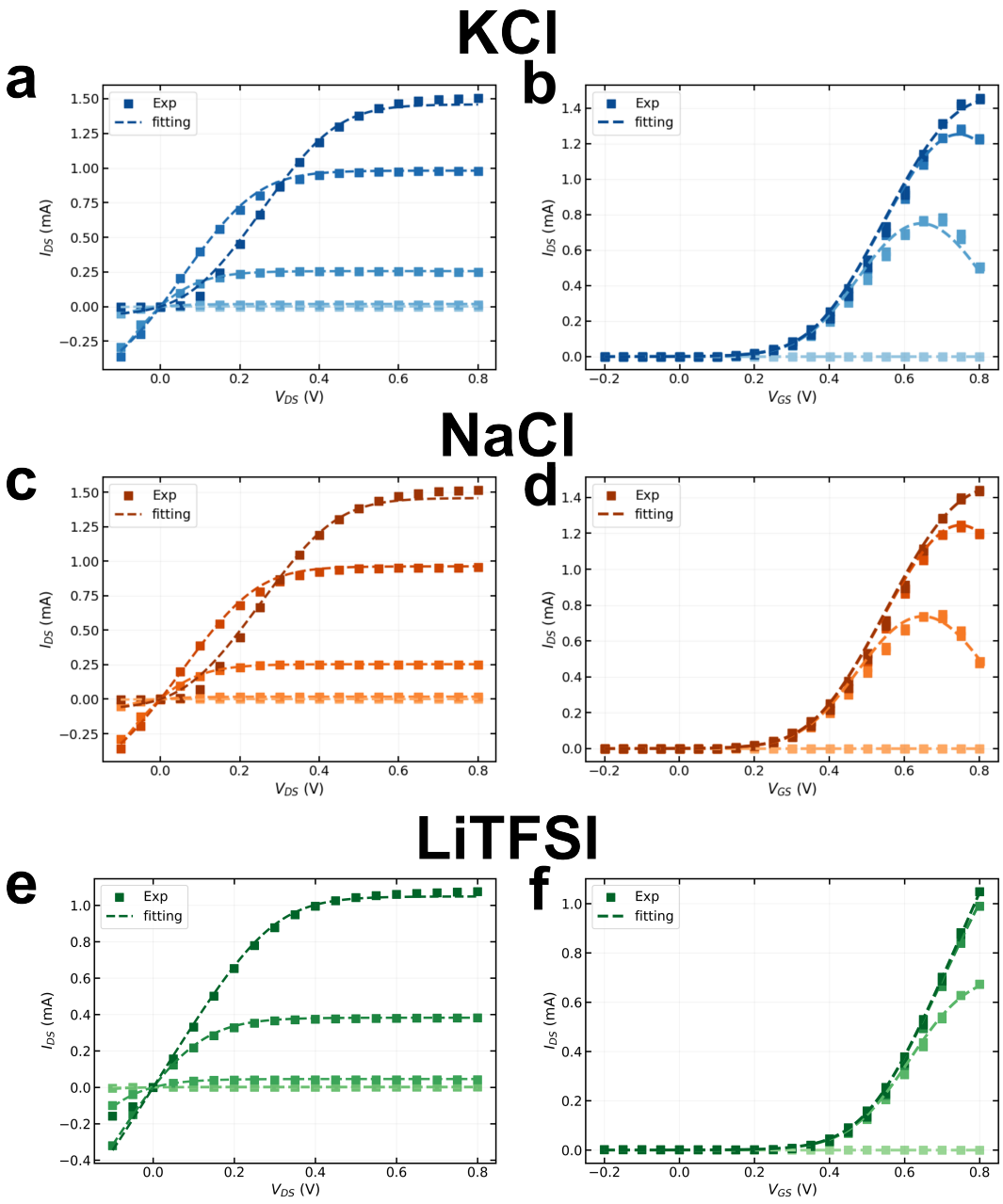

Figure S4. Fitting of our experimental data. **a.** Output and **b.** transfer curves for KCl 100 mM. **c.** Output and **d.** transfer curves for NaCl 100 mM. **e.** Output and **f.** transfer curves for LiTFSI 100 mM. The fitting was done with output curves, while transfer curves were back-calculated. For all curves $W = 300$ µm, $L = 300$ nm and $d = 120$ nm.

Table S3. Fitting parameters from figure S4.

Electrolyte	σ_1 (S/m)	ε_1 (V)	ε_2 (V)	γ	χ^2
KCl	(39 ± 3)	$-(0.38 \pm 0.01)$	$-(0.71 \pm 0.01)$	(0.39 ± 0.03)	2.65×10^{-8}
NaCl	(37 ± 3)	$-(0.38 \pm 0.02)$	$-(0.72 \pm 0.01)$	(0.39 ± 0.04)	4.18×10^{-8}
LiTFSI	(30.4 ± 0.5)	$-(0.51 \pm 0.01)$	$-(1.07 \pm 0.08)$	(0.37 ± 0.01)	5.27×10^{-9}

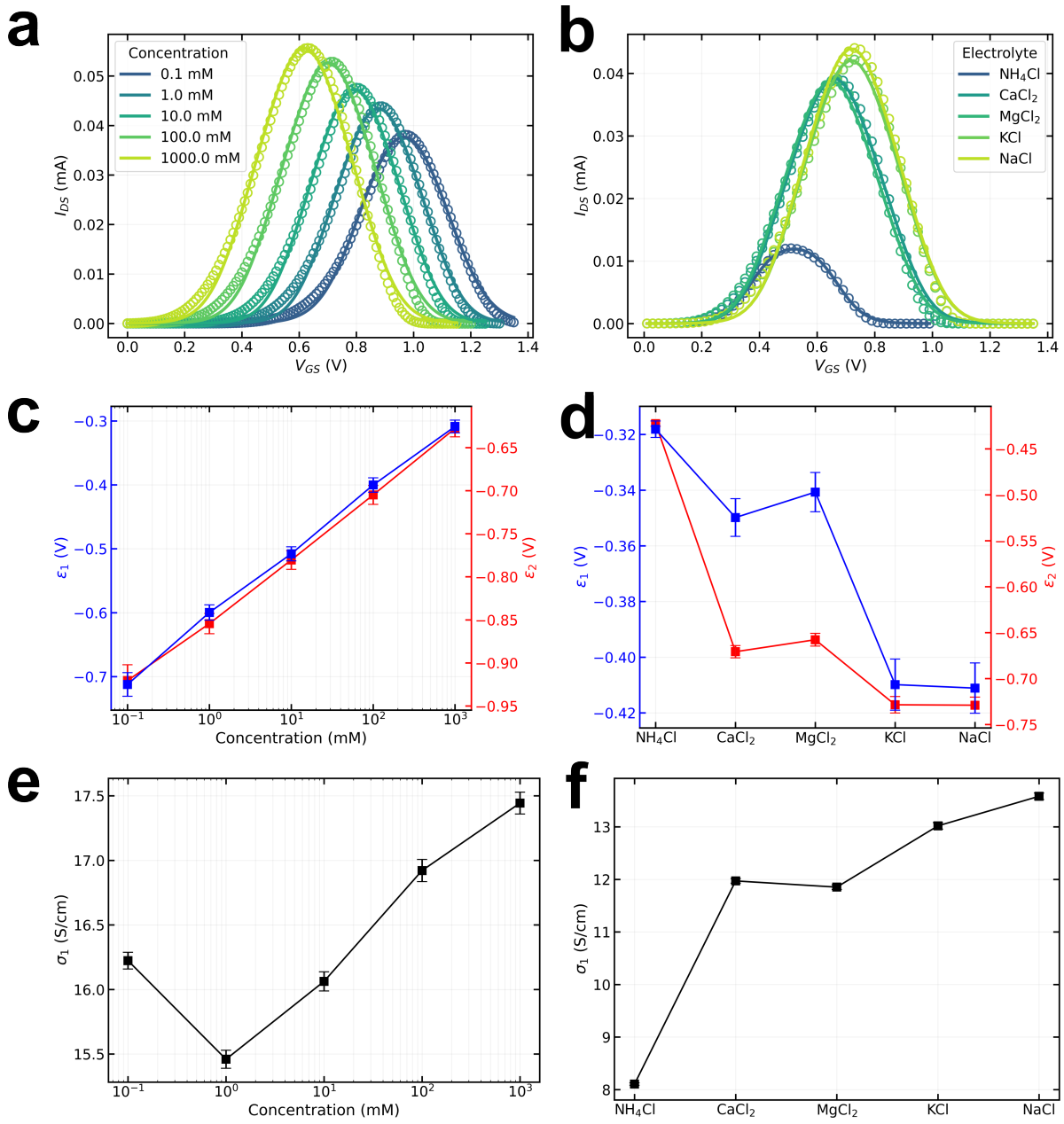

Figure S5. Fitting (solid lines) of public experimental data (hollow circles) from paper[3]. Transfer curves for **a.** different concentrations and **b.** different electrolytes. Extracted formal electrode potentials (**c.** and **d.**) and conductivity (**e.** and **f.**) for different electrolyte concentrations and salts, respectively. For all curves $V_{DS} = 0.3$ V, $W = 40$ µm, $L = 6$ µm and $d = 20$ nm.

Table S4. Fitting parameters from figure S5b.

Electrolyte	σ_1 (S/m)	ε_1 (V)	ε_2 (V)	γ	χ^2
NH_4Cl	(575 ± 2)	$-(0.29 \pm 0.01)$	$-(0.45 \pm 0.01)$	(0.74 ± 0.03)	1.71×10^{-2}
$CaCl_2$	(1197 ± 4)	$-(0.35 \pm 0.01)$	$-(0.67 \pm 0.01)$	(0.55 ± 0.04)	4.98×10^{-2}
$MgCl_2$	(1185 ± 5)	$-(0.34 \pm 0.01)$	$-(0.66 \pm 0.01)$	(0.57 ± 0.05)	5.42×10^{-2}
KCl_2	(1302 ± 6)	$-(0.41 \pm 0.01)$	$-(0.73 \pm 0.01)$	(0.53 ± 0.05)	8.42×10^{-2}
$NaCl_2$	(1358 ± 6)	$-(0.41 \pm 0.01)$	$-(0.73 \pm 0.01)$	(0.54 ± 0.05)	8.17×10^{-2}

Table S5. Fitting parameters from figure S5a.

Concentration (mM)	σ_1 (S/m)	ε_1 (V)	ε_2 (V)	γ	χ^2
0.1	(1622 ± 6)	$-(0.71 \pm 0.02)$	$-(0.92 \pm 0.02)$	(0.45 ± 0.04)	5.95×10^{-2}
1	(1546 ± 7)	$-(0.60 \pm 0.01)$	$-(0.85 \pm 0.01)$	(0.54 ± 0.05)	7.16×10^{-2}
10	(1606 ± 7)	$-(0.51 \pm 0.01)$	$-(0.78 \pm 0.01)$	(0.54 ± 0.05)	7.15×10^{-2}
100	(1692 ± 9)	$-(0.40 \pm 0.01)$	$-(0.70 \pm 0.01)$	(0.51 ± 0.05)	8.64×10^{-2}
1000	(1744 ± 4)	$-(0.31 \pm 0.01)$	$-(0.63 \pm 0.01)$	(0.50 ± 0.05)	7.74×10^{-2}

References

1. Feitosa, B. d. A., Torres, B. B. M., Luginieski, M., Coutinho, D. J. & Faria, G. C. Non-ideal nernstian behavior in organic electrochemical transistors: fundamental processes and theory. *Mater. Horiz.* **11**, 6007–6018, DOI: 10.1039/D4MH00758A (2024).

2. Xu, K. *et al.* On the origin of seebeck coefficient inversion in highly doped conducting polymers. *Adv. Funct. Mater.* **32**, 2112276, DOI: https://doi.org/10.1002/adfm.202112276 (2022). https://advanced.onlinelibrary.wiley.com/doi/pdf/10.1002/adfm.202112276.

3. Harikesh, P. C. *et al.* Ion-tunable antiambipolarity in mixed ion–electron conducting polymers enables biorealistic organic electrochemical neurons. *Nat. Mater.* **22**, 242–248, DOI: 10.1038/s41563-022-01450-8 (2023).